E-Journal of Advanced Maintenance Vol.5 No.2 (2013) 121-127
Japan Society of Maintenology

Partial CT and Structural Analysis with 950 Kev/3.95 Mev X-Band Linac X-Ray Sources

Wenjing Wu[1,*], Haitao Zhu[1], Ming Jin[1], Katsuhiro Dobashi[1], Takesi Fujiwara[1], Mitsuru Uesaka[1], Joichi Kusano[2], Naoki Nakamura[2], Eiji Tanabe[2], Hideyuki Sunaga[3], Yoshie Otake[3]

[1]*The University of Tokyo, Department of Nuclear Engineering and Management, Room213, Nuclear Annex, 2-11-16 Yayoi, Bunkyo-ku, Tokyo, 113-0032, Japan*
[2]*Accuthera Inc., 2-7-6 Kurigi, Asaoku, Kawasaki, 215-0033, Japan*
[3]*Riken, 2-1 Hirosawa, Wako, Saitama 351-0198, Japan*

ABSTRACT

For the purpose of applying CT by X-band linac to NDE of bridges, NPPs and architectures, relative experiment and imaging reconstruction is studied. Three reconstruction algorithms of FBP, ART and SART are compared in consideration of partial projection situation because possible scanning is confined to smaller than 180° angle and a few translations during inspection. CT system with linacs under 4Mev for scanning will work on-site as Japanese law permitted. Moreover, 3D model can be built based on reconstructed images to evaluate load-bearing performance of bridges with VCAD system.

KEYWORDS

CT, Linacs, X-ray, NDE

ARTICLE INFORMATION

Article history:
Received 13 November., 2012
Accepted 3 June., 2013

1. Introduction

Recent years, many bridges built around 1950s-1970s in Japan, which have served nearly more than 50 years, are facing safety problems caused by aging. [1] Some collapse accidents even happened due to degradation. In order to find an effective way for inspection, CT system using X-band linac scanning as NDE method is under development. [2, 3] Complying with Japanese law that accelerator under 4MeV can be taken out of controlled area for on-site inspection, we will use 3.95MeV linac as X-ray emitter.

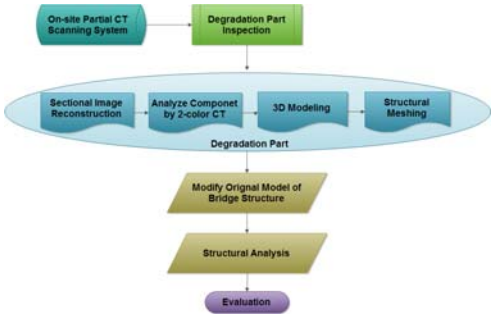

Fig. 1. Schematic view of partial CT inspection system

Focusing on degradation part, the projection data obtained by scanning with linac can reconstruct sectional images to inspect interior structure. Some factors mainly effect the load bearing performance of bridge would be examined, such as inner steel soundness situation like erosion and crack, as well as holes. Since iron and iron dioxide show different density and attenuation character, atomic number can be estimated by 2-colored CT to check the erosion thickness. What's more, in order to evaluate the mechanical characters of structure influenced by degradation, original 3D model of bridge can be

*Corresponding author, E-mail: wu@nuclear.jp

modified to substitute degradation module with new mesh, which is built with reconstructed sectional images. VCAD software, developed by Riken, Japan, is adopted for modeling and further structural analysis. [4]

However, only limited range of projection data is available in on-site inspection, since the bridge shape confines the possible scanning angle. Considering acquiring as many data as possible to improve reconstruction quality, scanning mood contains both rotation and translation, as indicated in figure 2. In section 2, three fundamental reconstruction algorithms are studied considering effects of partial projection. Then reconstruction results with experimental data are compared in section 3. The following section gives the example of modeling and structural analysis by VCAD, to explain the last step of our on-site partial CT inspection system.

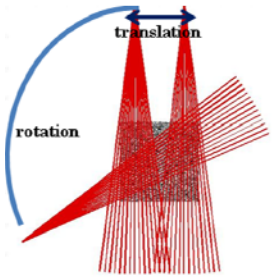

Fig. 2. Scanning mood with rotation and translation

2. Reconstruction Algorithms for Limited Projection Data

The Filtered Back Projection (FBP) [5] and Algebraic Reconstruction Technique (ART) [6, 7] are two most fundamental and popular algorithms. Simultaneous Algebraic Reconstruction Technique (SART) [8] is developed from ART as a better version. Their methods are briefly introduced referred to former achievements and the reconstruction results are also compared and analyzed.

2.1. Reconstruction Algorithm Theories

2.1.1 Filtered Back Projection (FBP)

FBP as an analytic reconstruction algorithm is based on Radom transform. According to Fourier Slice Theorem, the one-dimensional Fourier transform of a parallel projection is equal to a slice of two-dimensional Fourier transform of the original function. Therefore, it is possible to estimate the original function by performing a two-dimensional inverse Fourier transform with the given projection data. [9, 10]

2.1.2 Algebraic Reconstruction Technique (ART)

ART is an iterative reconstruction technique. The iteration process is run for solving the equation

$$Ax = b \tag{1}$$

where x is the value at each pixels denoting the density property information of the measured object and b the projection data measured through scanning. [11] A is the integration matrix. ART adopts Kaczmarz method [12, 13] to solve the above equation:

$$x_{k+1} \leftarrow x_k + \lambda_k \frac{b_i - < a_i, x_k >}{\|a_i\|_2^2} a_i \tag{2}$$

Here $0 < \lambda_k < 2$.

2.1.3 Simultaneous Algebraic Reconstruction Technique (SART)

SART is developed from ART and “simultaneous” is in the sense that all the equations in (1) is

used simultaneously in one iteration to correct errors in all ray-sum equations. [8, 13] Iterative procedure goes like this:

$$x_{k+1} \leftarrow x_k + \lambda_k D_r^{-1} A^T D_c^{-1} (b - Ax^k) \tag{3}$$

Here D_r and D_c are defined as

$$D_r = diag(\|a^i\|_1), \qquad D_c = diag(\|a_j\|_1). \tag{4}$$

2.2. Simulation Result Comparison

A well-known Shepp-logan Phantom image of 100×100 pixels is reconstructed with limited projection data of different angle range by three algorithms mentioned above, in the case of without noise or with 5% white noise. The Signal/Noise Ratio (SNR) derived from exact image and reconstructed image are listed in table 1, as well as consumed computational time. Table 2 gives the counterpart results when reconstructing only region of interest under partial scanning condition.[10, 13]

Table 1 SNR and computational time comparison

Algorithm		FBP		ART		SART	
Term	Projection angle	Without noise	With 5% noise	Without noise	With 5% noise	Without noise	With 5% noise
SNR(dB)	180	2.89	2.81	20.4	12.2	18.8	13.5
	120	1.57	1.51	6.47	5.72	6.99	6.16
	90	0.549	0.502	4.31	4.09	4.8	4.14
TIME(s)	180	0.050114	0.049461	8.637209	8.811013	1.041747	0.984081
	120	0.033475	0.033555	3.853454	3.878226	0.436340	0.458855
	90	0.025466	0.024838	2.194112	2.200374	0.273049	0.265118

Table 2 SNR comparison for ROI

Algorithm		FBP		ART		SART	
Term	Projection angle	Without noise	With 5% noise	Without noise	With 5% noise	Without noise	With 5% noise
SNR(dB)	180	12.1	11.2	22.2	13.2	25.1	13.4
	120	8.01	7.58	10	9.1	11.1	9.37
	90	5.75	5.49	7.04	6.68	8.63	7.54

Artifacts and blurring get serious as projection angle decreases, especially around edge. According to the comparison, ART and SART can reach higher SNR than FBP even under partial scanning condition, mainly due to better edge preserving ability. SART is faster than ART. However, FBP shows a significant advantage in computational time than the other two algorithms, due to no need for iterative process, which would be quite helpful when reconstructing large amount of sectional images during real inspection. It also costs quite large memory for ART and SART because necessary projection data should all be available before the iterative reconstruction starts. [14-16] Moreover, salt and pepper noise is easy to appear in image reconstructed by iterative algorithms, which made it not so effective to improve image quality further by more iteration loops, especially for noisy data. [8] FBP gives comparatively smoother image. Actually, the SNR of FBP reconstruction for ROI is still acceptable, especially for noisy data. Those demerits made FBP become a better choice for on-site inspection. Further study is carried out with experimental data in next section.

3. Reconstruction with Experimental Data

3.1 Test Experiment

Test experiment is implemented with a small concrete cylinder sample (h: 100mm, Φ: 100mm) containing inner steel rods. Additionally, one aluminum sample, one iron sample and a battery are

attached on top of the concrete sample for comparison. For test, 950 keV linac is adopted as X-ray emitter and a panel detector is used. The sample placed on a rotation stage to acquiring data from different angle directions. Through transmitted image in figure 3, two inner steel rods, flat and inclined, can be well seen.

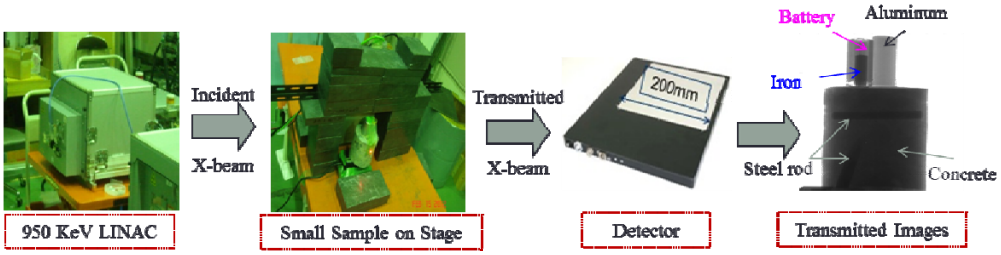

Fig. 3. Scanning experiment layout and transmitted image

3.2 Reconstruction Results

Sectional image of the slice positioned at the flat steel rod is reconstructed to 256×256 pixels images, as showed in figure 4. Results of different algorithms and projection angle are compared. The pixel value of horizontal line at middle is charted in figure 5. [10, 13]

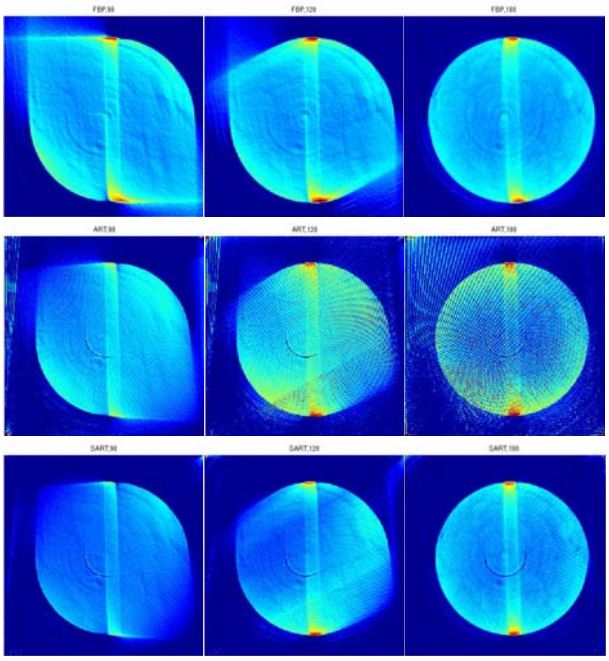

Fig. 4. Reconstructed sectional image
(Rows from upper to lower: reconstructed by FBP, ART and SART;
Rows from left to right: 90°, 120° and 180° projection data.)

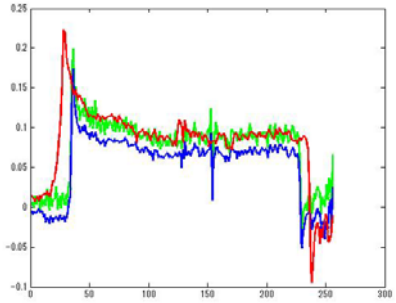

(a)

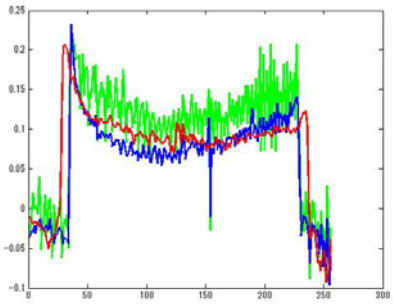

(b)

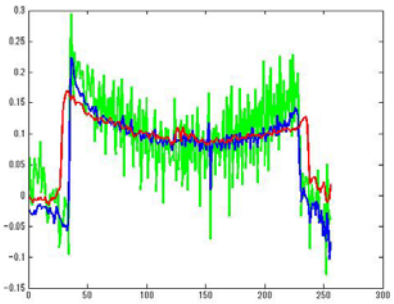

(c)

Fig. 5. Pixel value of horizontal line
(FBP, ART and SART are indicated by blue, green and red line relatively;
a is for 90° projection data, b 120° and c 180° .)

Although artifacts and blurring affect edge preserving significantly as projection angle decreased, inner steel rod is still discernible. Steel rod shows lighter color in center than outer mainly due to scattering X-ray inside concrete. However, ART suffers much salt and pepper noise generated during iteration process which decreased the image quality seriously, referring to figure 4 and 5. Due to the iterative process, ART takes more than 20 min to calculate one slice with 180° projection data, SART 3 min, much too long compared with FBP, which only needs 1 sec. Furthermore, better material resolution of FBP is illustrated in figure 5. Since it's of significant importance to distinguish steel and concrete for our detection target and fast reconstruction speed is demanded for on-site work, FBP is finally adopted as reconstruction algorithm in our system to complete later procedure.

4. Mechanical Analysis

With 60 slices reconstructed by FBP for the concrete sample from top to bottom, 3D model of the sample is built and mechanical analysis process is tested by VCAD system. [4]

4.1 3D Model

VCAD is software capable of building 3D model based on slice images through discerning different material in images by color contrast, so accurate and apparent color discrimination of inner structure is highly demanded to build correct model. However, too much noise caused by scattering X-ray affects the image quality that the software cannot distinguish color exactly between steel and concrete. Total variation regularization is tried which is capable at reducing noise while maintaining clear boundary. [17] As showed in figure 6, although the whole image is smoothed in general with good edge preserving performance, the middle part of the steel rod located deep inside the concrete is still showing very light color. In order to avoid vague distinction between steel and concrete in 3D model, manual processing is carried out to condense steel color before modeling. Afterwards, the 3D model and mesh is built as showed in figure 8.

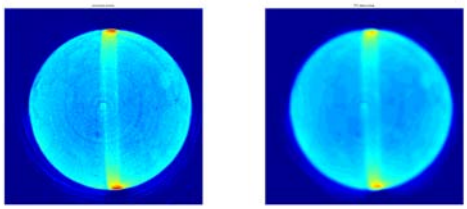

(a) (b)

Fig.6 Total Variation regularization
(a: reconstructed image; b: denoising result)

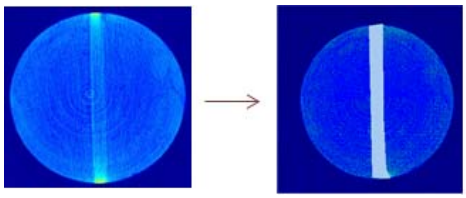

Fig.7 Manual processing before modeling

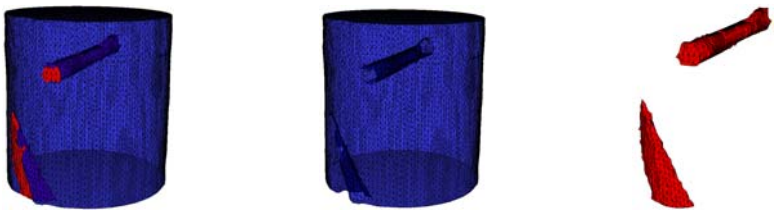

(a) (b) (c)

Fig.8 Modeling and meshing
(a: 3D mesh of sample; b: concrete; c: steel)

4.2 Mechanical analysis

For simulation, 50,000N force is evenly loaded on top surface of the sample with bottom fixed. Material parameters are showed in table 3. The obtained simulation results are well complied with theoretical results. Figure 9 give the equivalent stress distribution.

Table 3 Material parameters

Material	Young's modulus (MPa)	Poisson's ratio
Concrete	28000	0.15
Steel rod	219620	0.3

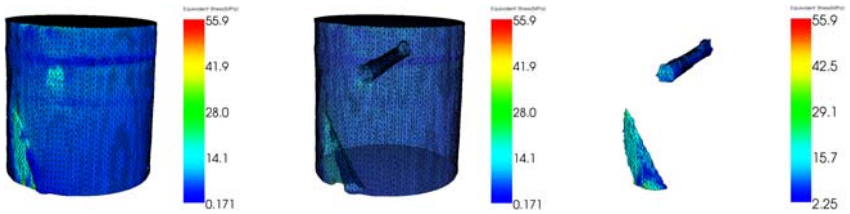

(a) (b) (c)

Fig.9 Equivalent stress (MPa)
(a: sample; b: concrete; c: steel)

5. Conclusion

Three algorithms are compared and FBP is adopted for on-site CT inspection system in view of faster reconstruction speed and better material resolution. Although the mechanical evaluation is successfully conducted after manual processing to sectional images in the test, measures for reducing scattering X-ray noise is still an unavoidable problem. Solution is under study as trying a line sensor

with collimator firstly to reduce scattered X-ray and improve imaging quality. Additionally, 2-color CT can also be implemented with the line sensor because there is a high-energy detector and a low detector compacted inside. Methods about atomic number estimation would be developed.

References

[1] M. O. Takashi TAMAKOSHI, Takenobu KITAMURA: "Annual Report of basic dataon Road Structures in FY", 28, 2009 Oct.
[2] M. Uesaka, T. Natsui, K. Lee, K. Dobashi, T. Yamamoto, T. Fujiwara, H. Zhu, K. Demachi, E. Tanabe, M. Yamamoto, N. Nakamura, J. Kusano, T. Higo, S. Fukuda, M. Yoshida and S. Matsumoto: "950keV, 3.95MeV and 6MeV X-band linacs for nondestructive evaluation and medicine", (2011), Nuclear Instruments and Methods in Physics Research Section A: Accelerators, Spectrometers, Detectors and Associated Equipment, 657:1, 82-87.(2011)
[3] J. Ambrose and G. N. Hounsfield: "Computerized Transverse Axial Tomography", (1973), British Journal of Radiology, 46:542, 148-149.(1973)
[4] M. Akitake: "VCAD System: Advanced Software System for Production Engineering and Biological Research", (2010), JSCES, 15:2, 2309-2315.(2010)
[5] L. Shepp: "The Fourier Reconstruction of a Head Section", (1974), IEEE transactions on nuclear science, 21:3, 21.(1974)
[6] G. T. Herman, A. Lent and S. W. Rowland: "ART: Mathematics and applications: A report on the mathematical foundations and on the applicability to real data of the algebraic reconstruction techniques", (1973), Journal of Theoretical Biology, 42:1, 1-32.(1973)
[7] K. Tanabe: "Projection method for solving a singular system of linear equations and its application", (1971), Numer. Math., 17:203-214.(1971)
[8] A. H. Andersen and A. C. Kak: "Simultaneous Algebraic Reconstruction Technique (SART): A superior implementation of the ART algorithm", (1984), Ultrasonic Imaging, 6:1, 81-94.(1984)
[9] M. S. A C. Kak, Principle of Computerized Tomographic Imaging, IEEE, New York, 1999,
[10] G. Peyre: "The Numerical Tours of Signal Processing - Advanced Computational Signal and Image Processing", (2011), IEEE Computing in Science and Engineering, 13:4, 94-97.(2011)
[11] M. Beister, D. Kolditz and W. A. Kalender: "Iterative reconstruction methods in X-ray CT", (2012), Physica Medica, 2012)
[12] S. Kaczmarz: "Angenäherte auflösung von systemen linearer gleichungen", (1937), Bull.Acad. Pol. Sci. Lett. A, 6:8A, 355-357.(1937)
[13] P. C. Hansen and M. Saxild-Hansen: "AIR Tools — A MATLAB package of algebraic iterative reconstruction methods", (2012), Journal of Computational and Applied Mathematics, 236:8, 2167-2178.(2012)
[14] D. Fleischmann and F. E. Boas: "Computed tomography-old ideas and new technology", (2011), European Radiology, 21:3, 510-517.(2011)
[15] X. C. Pan, E. Y. Sidky and M. Vannier: "Why do commercial CT scanners still employ traditional, filtered back-projection for image reconstruction?", (2009), Inverse Problems, 25:12, 2009)
[16] G. Wang, H. Y. Yu and B. De Man: "An outlook on x-ray CT research and development", (2008), Medical Physics, 35:3, 1051-1064.(2008)
[17] A. Chambolle: "An Algorithm for Total Variation Minimization and Applications", (2004), Journal of Mathematical Imaging and Vision, 20:1-2, 89-97.(2004)